

Functional MRI Reveals the Critical Role of Broca's Area in Speech Sound Disorders

X. Chen^{1,2}, B. Lewis³, A. Hansen³, L. Freebairn³, and J. Tkach^{1,2}

¹Radiology, Case Western Reserve University, Cleveland, Ohio, United States, ²Case Center For Imaging Research, CWRU, Cleveland, Ohio, United States,

³Communication Sciences, CWRU, Cleveland, Ohio, United States

Introduction: Speech sound disorders (SSD) are the largest group of communication disorders observed in children requiring special education services. However, to date, the neurological origin of SSD has not been researched extensively. We conducted a functional MRI (fMRI) study using the HUSH (Hemodynamics Unrelated to Sounds from Hardware^[1]) technique on 6 participants with SSD history of unknown etiology in comparison to 9 age-matched controls during an overt non-word repetition task. Preliminary results demonstrate significant under-activation in Broca's area, an area known to be crucial for speech production, for the patient group, suggesting the critical role Broca's area plays in SSD.

Methods: 1) Data Acquisition: MRI data was acquired on 15 participants (6 SSDs with age range of 9-18ys and 9 age-matched controls) on a 4T Bruker scanner. For each participant, a high resolution 3D T1 weighted MPRAGE anatomical scan was acquired for the purpose of spatial normalization, followed by a functional run using a gradient echo EPI sequence with parameters TR/TE=2s/20ms, Flip Angle=76.8°. A multi- gradient echo reference scan was also acquired for the purpose of correcting the EPI data for Nyquist ghosting and geometric distortion^[2]. The fMRI data was collected using the HUSH technique, a clustered fMRI design with the paradigm illustrated in **Fig.1**. Each two-phase epoch of the HUSH design consisted of (1) a 6s scanner silent time window, during which the participants were asked to rest or to perform overt repetition of a non-word presented auditorily, and (2) a 6s period during which 3 EPI volumes covering the entire brain were acquired. In each fMRI run, ten repetition epochs alternated with ten

Gradients/Acq	Silent	Acquire	Silent	Acquire	Silent	Acquire	Silent	
Task	rest	X	repeat	X	rest	X	repeat	
Auditory Stim	OFF	OFF	ON	OFF	OFF	OFF	ON	
Interval Time	6s	6s	6s	6s	6s	6s	6s	
Running Time	6s	12s	18s	24s	30s	36s	42s	

Fig. 1. Diagram of the HUSH-fMRI acquisition

rest epochs, for a total scan time of $20 \times (12 \text{ seconds/epoch}) = 4 \text{ minutes}$. The non-word list consisted of 6 single syllable words and 4 2-syllable words taken from the WRMT-R (form H)^[3]. To establish T1 equilibrium, an additional 6s acquisition period (3 EPI volumes collected) was performed at the onset of fMRI collection. **2) Data Analysis:** For each participant, the EPI data were initially corrected for geometric distortion and motion. The first 3 volumes were discarded. The remaining corrected volumes were then grouped according to 1st, 2nd, or 3rd scan of each data acquisition period, and further subdivided into control and task subsets. A paired t-test was computed on a voxel wise basis between the condition pair. A Z-score was then derived from the t-score as the individual result. At the group level, images from individual participants were spatially normalized to Talairach space. For both normative and SSD cohorts, a random effect result was computed with appropriate corrections for multiple comparisons and clustering. All image processing was completed using Cincinnati Children's Hospital Image Processing Software (CCHIPS©).

Results and Discussion: **Fig. 2** illustrates the comparison of random effect results between the control group (**Fig. 2A**) and the SSD group (**Fig. 2B**), together with a typical SSD individual result (**Fig. 2C**) in the contrast of non-word repetition vs. silent control. Consistent Z-score threshold of 2.5 (corresponding to uncorrected $p \leq 0.006$) was applied to all results. Voxels that did not occur in a cluster of at least 5 suprathreshold voxels (approximately 210 mm^3) were disregarded. For the control group (**Fig. 2A**), activation can be seen in both Broca's and Wernicke's areas with the expected overall left hemispheric dominance. For the SSD cohort (**Fig. 2B**), although activation is found in Wernicke's area, Broca's area demonstrated substantially reduced activation (see the yellow circles).

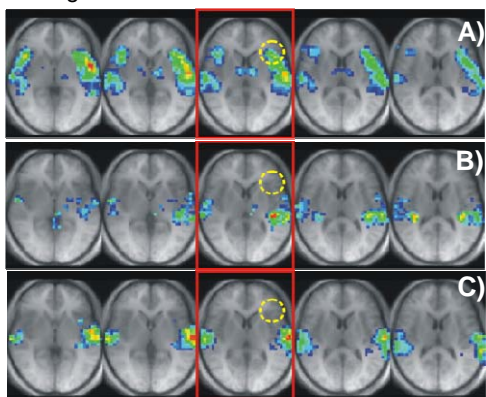


Fig. 2. Random effect group results for both controls (**Fig. 2A**) and participants with SSD history (**Fig. 2B**), together with the individual result from a typical SSD participant (**Fig. 2C**). All results were spatially normalized into the TLRC space and illustrated in transverse AC-PC orientation at TLRC $Z = +1\text{mm}$ to $Z = +13\text{mm}$ at an interval of 3mm. A ROI in Broca's was highlighted using yellow circle in the slice with TLRC $Z = +7\text{mm}$ (red box). Image Right=Brain Left

Notably, the activation patterns observed in the SSD group closely matched those demonstrated by affected KE family (a family demonstrating a heritable orofacial apraxia and associated SSD) members during the performance of an overt word repetition task^[4]. This interesting finding may partially reveal the neurologic origin of SSD and deserves further investigation. Recognizing the potential heterogeneity in the behavioral phenotype across the 6 SSD participants and possibly insufficient power due to the small sample size, the individual result of a representative SSD participant is also presented in **Fig. 2C** with findings similar to the group analysis.

Conclusion: This study demonstrates that fMRI using overt non-word repetition tasks is a powerful tool to investigate the neurologic origins of SSD. The preliminary results suggest the critical role Broca's area may play in SSD.

References: [1] Schmithorst, VJ, et al (2004), *MRM*, 51, p399; [2] Schmithorst, VJ, et al (2001), *IEEE TMI*, 20, p535; [3] Woodcock, R (1987), *WRMT -revised*, American Guidance Services Inc; [4] Liegeois, F, et al (2003), *Nat Neurosci*, 6, p1230.

Acknowledgements: The authors thank Drs. Scott Holland, Vince Schmithorst and Prasana Karunanayaka for providing the HUSH sequence and CHIPS software. We also thank Jack Jesberger for his assistance in data acquisition. This work was partially supported by ONDCP (project #: DABK 39-03-C-0061).